Pol. J. Environ. Stud. Vol. XX, No. X (XXXX), 1-13
DOI: *10.15244/pjoes/210391* ONLINE PUBLICATION DATE: 2025-12-09

Review

Electrolyte Leakage and Seepage Mechanism of Electrochemical Energy Storage Stations in Cold Regions: A Review

An Tao[1], Zhaohui Shi[1], Lei Zhang[1], Sen Hu[1], Bo Tan[2, 3°*]

[1]PowerChina Huadong Engineering Corporation Limited, Hangzhou 311122, China
[2]State Key Laboratory of Hydraulics and Mountain River Engineering, Chengdu 610065, China
[3]College of Water Resource and Hydropower, Sichuan University, Chengdu 610065, China

Received: 26 June 2025
Accepted: 7 September 2025

Abstract

As global deployment of electrochemical energy storage accelerates to support renewable energy integration, infrastructure in cold regions faces unique electrolyte leakage hazards that threaten operational safety and environmental integrity. This review synthesizes critical mechanisms governing electrolyte seepage under subzero conditions, where cryogenic temperatures induce phase separation (e.g., salt precipitation in Li-ion carbonates, vanadium hydrate crystallization in flow batteries) and material embrittlement, exacerbating containment failure. Leaked electrolytes exhibit multiphase transport dynamics dominated by freeze-thaw cycles: ice formation restricts vertical leaching but generates anisotropic migration pathways through unfrozen brine channels and frost-heaved soil cracks, while thermal gradients drive directional contaminant spread via solute exclusion and Soret effects. Physically based models (SHAW, CoupModel, Hydrus-1D) simulate these coupled thermo-hydro-chemical processes, integrating Clapeyron-driven phase transitions and non-Arrhenius ion transport scaling. However, knowledge gaps persist in quantifying interfacial electrochemistry at ice-electrolyte boundaries and predicting multicomponent cross-drag in frozen matrices. The analysis establishes a foundation for designing cryogenic-resilient containment systems, addressing urgent safety and environmental challenges for energy storage in cold climates.

Keywords: electrochemical energy storage, cryogenic electrolyte leakage, freeze-thaw cycling, anisotropic transport, contaminant migration

Introduction

Electrochemical energy storage (EES) systems are pivotal for stabilizing renewable energy integration and enhancing grid resilience amid global decarbonization efforts [1, 2]. Rapid deployment has expanded into cold regions worldwide, with projects like Norway's Svalbard microgrid and large-scale installations in high-latitude/snowbelt regions highlighting this trend, driven by land availability and renewable proximity [3, 4]. However, subzero conditions introduce unique hazards: electrolyte leakage, triggered by material

* e-mail: tanbo@scu.edu.cn
°ORCID iD: 0000-0001-6931-6984

embrittlement (e.g., fluorinated rubber seal failure below –20ºC) and phase transitions, interacts with frozen soils through freeze-thaw dynamics whose environmental impacts remain insufficiently characterized [2, 5]. This creates anisotropic contaminant pathways via brine channels and frost-heaved cracks, posing unresolved environmental and safety risks despite accelerated infrastructure growth.

The performance and safety of electrochemical energy storage systems in cold regions are fundamentally constrained by electrolyte phase transitions and material degradation. Organic carbonate-based electrolytes (e.g., EC/DMC mixtures) in lithium-ion batteries exhibit severe viscosity surges and $LiPF_6$ salt precipitation below –20ºC, while vanadium sulfate electrolytes in flow batteries form crystal hydrates ($VOSO_4 \cdot 3H_2O$) below –5ºC, impairing ion mobility and system integrity [2, 6]. Concurrently, structural materials such as fluorinated rubber seals lose elasticity at -20°C, and aluminum current collectors undergo ductile-to-brittle transitions, exacerbating leakage risks [7]. Once leaked, cryogenic conditions alter contaminant transport: ice layers initially restrict vertical penetration, but repeated freeze-thaw cycles generate frost-heave cracks that redirect electrolytes laterally, creating localized pollution hotspots [8, 9]. These coupled physicochemical processes remain poorly quantified, hindering predictive modeling of long-term environmental impacts.

Electrolyte leakage in cold environments triggers complex multiphase interactions that amplify environmental hazards. Phase instability under freeze-thaw cycles promotes dendritic crystal growth and microcrack formation in containment materials, accelerating structural degradation. Chemically, low temperatures exacerbate reactivity, $LiPF_6$ hydrolysis releases corrosive HF gas more rapidly, while vanadium ions exhibit heightened oxidation potential, destabilizing soil colloids [10, 11]. Transport processes become highly anisotropic: solute exclusion during ice formation concentrates brines along freezing fronts, while thermal gradients drive Soret-induced directional migration of contaminants [9, 12]. These coupled phenomena create spatially heterogeneous pollution patterns, complicating remediation efforts in permafrost-affected regions.

While existing studies have attempted to synthesize the mechanisms of electrolyte leakage in cold environments by examining phase transitions and transport behaviors, critical knowledge gaps persist that hinder predictive modeling and risk mitigation. The electrochemical dynamics at ice-electrolyte interfaces, including low-temperature ion transport through SEI layers, remain poorly understood due to experimental limitations in cryogenic operando characterization [6, 13]. Furthermore, the cross-coupling effects of multicomponent electrolyte systems, particularly temperature-dependent drag coefficients, are rarely quantified, impeding accurate simulations of solute redistribution during freeze-thaw cycles [12]. Current coupled models of frozen soil-contaminant interactions also lack validation, especially in heterogeneous soils where preferential flow dominates contaminant dispersion [8, 9].

Moreover, research on the environmental fate of leaked electrolytes in cold regions remains limited, with few studies addressing the synergistic effects of thermal gradients, phase separation, and biogeochemical reactions. Among the limited literature on this topic, only a small fraction systematically integrates experimental data (e.g., soil column tests, molecular dynamics) with field-scale models (e.g., SHAW, CoupModel) to bridge molecular-scale mechanisms with ecosystem-scale impacts [7, 11]. This review argues that advancing the fundamental understanding of cryogenic electrolyte percolation, from phase transitions to anisotropic transport, will pave the way for safer energy storage designs in cold climates. By synthesizing interdisciplinary insights, this work aims to identify key pathways for mitigating leakage risks while highlighting unresolved challenges in material science, electrochemistry, and environmental hydrology.

Results and Discussion

Characteristics and Distribution of Global Electrochemical Energy Storage

The Development History of Electrochemical Energy Storage

Electrochemical energy storage traces its roots to pioneering 18th-19th century innovations, including Luigi Galvani's bioelectricity discoveries and Alessandro Volta's first battery (1800), followed by Gaston Planté's rechargeable lead-acid battery (1859), which fueled early telegraphy and electric vehicles [14]. The 20th century introduced nickel-cadmium systems (1899) and breakthroughs like John B. Goodenough's lithium cobalt oxide (1980), leading to Sony's commercialization of lithium-ion (Li-ion) batteries in 1991, a milestone that transformed portable electronics. By the 21st century, Li-ion dominated energy storage with high energy density (300-400 Wh/m^3), 90% efficiency, and an 89% cost reduction, enabling grid-scale projects like China's 20 MW Zhangbei station and electric vehicle proliferation[15, 16]. Concurrently, vanadium flow and sodium-sulfur systems addressed grid challenges despite technical limitations [3]. Modern advancements prioritize solid-state batteries, hybrid Li-ion-supercapacitor configurations, and sustainable cobalt-free cathodes, propelled by global decarbonization initiatives and AI-driven optimizations, solidifying electrochemical storage as essential for renewables integration and grid resilience [17, 18].

Global Deployment Patterns and Case Studies of Electrochemical Energy Storage

In the context of the global transition toward renewable energy integration and grid stability enhancement, electrochemical energy storage systems have been widely deployed across diverse geographical and climatic conditions, serving as critical infrastructure to balance supply-demand dynamics and support renewable energy penetration [19]. As shown in Fig. 1, Japan's Hokkaido Electric Power Network (HEPCO) pioneered grid-scale VRFB deployment with a 17 MW/51 MWh system at Minami-Hayakita Substation, centralizing renewable fluctuation management and lowering operational costs. In the United States, the Moss Landing Power Plant exemplifies hybrid energy infrastructure, combining natural gas generation with a 630 MW/2,500 MWh battery facility, the world's largest as of 2025, to store solar surplus and stabilize California's grid. Canada's Oneida Energy Storage (250 MW/1,000 MWh) and Germany's Aquila Clean Energy project (50 MW/100 MWh) highlight advancements in lithium-ion technology, optimized for wholesale market trading and cobalt-free sustainability, respectively.

China has emerged as a pivotal player in grid-scale electrochemical storage deployment, exemplified by landmark projects such as the Dalian Hengliu vanadium redox flow battery (VRFB) system (200 MW/800 MWh), the world's largest since 2016, and the Dongying Jinhui facility (500 MW/1,000 MWh), integrating high-density lithium iron phosphate cells to reduce land use by 25% and offset 101,000 tons of coal annually. Rapid infrastructure expansion is evident in extreme environments like Qinghai's Chaidamu Basin, where a 270 MW/1,080 MWh shared storage plant achieved grid synchronization within 25 days using liquid-cooled systems. As shown in Fig. 2, by 2020, China's cumulative energy storage capacity reached 35.6 GW (18.6% of global capacity), with electrochemical storage (EES) surging to 3.27 GW, a 91.2% year-on-year increase driven by lithium-ion dominance (88.8% share). Post-2018 explosive growth, including a 316% installation spike that year, underscores China's alignment of technological scale-up with decarbonization strategies [20].

Notably, a significant proportion of these large-scale electrochemical storage installations are situated in cold climates where seasonal or perennial subzero temperatures prevail [2, 5]. While site selection often prioritizes land availability and renewable energy proximity, frigid environments introduce unique challenges in operational safety and environmental protection [21]. Unlike temperate regions, where electrolyte leakage primarily risks immediate soil infiltration, freezing conditions alter contaminant transport dynamics: frozen ground may temporarily restrict vertical leaching, whereas freeze-thaw cycles can enhance lateral spreading via ice lens formation and soil cracking. This physicochemical interplay between electrolytes (e.g., $LiPF_6$, vanadium species) and cryogenic soils remains understudied, despite its relevance to long-term groundwater protection.

Characteristics of Electrolytes in Cold Regions

Contemporary electrochemical energy storage systems primarily employ lithium-ion batteries (LiBs), vanadium redox flow batteries (VRFBs), sodium-sulfur (Na-S) batteries, and lead-acid batteries [22]. Each system features distinct electrolytes: (1) LiBs typically use organic carbonate-based solutions (e.g., $LiPF_6$ in EC/DMC mixtures), with ionic liquid or solid-state alternatives emerging [23]; (2) VRFBs rely on acidic vanadium sulfate (V^{2+}/V^{3+} in H_2SO_4) or chloride-based electrolytes [1]; (3) Na-S batteries utilize molten sodium and sulfur separated by a β-alumina solid electrolyte at high temperatures (~300ºC) [22]; (4) lead-acid systems contain aqueous sulfuric acid [23]. Hybrid configurations may integrate these electrolytes with additives to enhance conductivity or thermal stability [24].

In cold climates (<0ºC), electrolyte behavior deviates significantly from standard conditions. Organic LiB electrolytes exhibit viscosity surges (e.g., EC/DMC viscosity triples at –20ºC), reducing Li^+ diffusivity and fostering salt precipitation. VRFB electrolytes may form vanadium crystal hydrates (e.g., $VOSO_4 \cdot 3H_2O$) below –5ºC, impairing flowability [25]. Lead-acid undergoes freezing at ~–70ºC but faces conductivity decay above this threshold. Molten Na-S electrolytes require auxiliary heating to prevent solidification, raising operational costs. Such phase transitions and transport limitations heighten leakage risks during thermal cycling, as mechanical stress from repeated freezing/thawing can compromise battery seals [26].

Upon leakage, electrolyte-soil interactions in cold regions are governed by freeze-thaw dynamics. Organic LiB electrolytes (e.g., EC/DMC) resist immediate freezing due to low water affinity but exhibit multi-year persistence in soils, with hydrophobic components (e.g., $LiPF_6$) adsorbing to organic matter while polar solvents migrate downward during thaw phases [8, 27]. Acidic VRFB electrolytes destabilize soil colloids, accelerating metal leaching under freeze-thaw-induced cracking. H_2SO_4 rapidly depresses soil pH, enhancing heavy metal solubility, while ice formation temporarily confines its spread, creating localized contamination hotspots upon melting [28, 29]. Molten Na-S electrolytes solidify upon contact with cold soil, posing limited mobility but persistent alkalinity risks. Predictive modeling of these processes must account for cryogenic soil properties (e.g., ice saturation, permeability hysteresis) to assess long-term groundwater threats [30, 31].

Germany (Dahlem)
321 MW battery storage across six sites, using Saft's LFP technology; commercial operation expected by 2026.

Germany (Schleswig-Holstein)
50 MW/100 MWh cobalt-free battery system (2024), optimized for market trading and grid balancing.

Canada (Haldimand)
Grid-scale lithium-ion facility (250 MW/1,000 MWh, operational since 2023), doubling Ontario's storage capacity.

China (Dalian)
Vanadium redox flow battery (200 MW/800 MWh), operational since 2016, provides peak shaving and emergency power with high safety.

UK (Wiltshire)
Battery storage (150 MW), developed by Penso Power; first phase commissioned in 2020.

Finland (Uusikaupunki)
50 MW/100 MWh project utilizing Sungrow PowerTitan 2.0 liquid-cooled systems for harsh Arctic conditions.

China (Qinghai)
270 MW/1,080 MWh plant in extreme high-altitude conditions, achieving grid synchronization in 25 days using SunGrow PowerTitan systems.

Norway (Svalbard)
6 MW/7 MWh Saft system (2022) to replace coal power and stabilize grid in Arctic winters.

USA (Kenai Peninsula, Alaska)
93 MWh Tesla Megapack BESS (2022) replacing gas turbines, operating in sub-zero temperatures.

China (Nanjing)
User-side storage project (61 MW/123 MWh), utilizing advanced string-pod technology for industrial energy optimization.

Canada (Whitehorse)
Planned 7 MW/40 MWh project (post-2022) to reduce diesel reliance in northern Canada.

China (Guangdong)
New energy storage station in Guangdong-Hong Kong-Macao Greater Bay Area (300 MW), representing 20% of its regional capacity.

USA (California)
Edwards & Sanborn Solar + Storage. Combined 864 MW solar + 3,287 MWh battery storage (2023), large hybrid project of its kind in the U.S.

South Africa (Northern Cape)
Hybrid plant (540 MW solar + 225 MW/1,140 MWh storage), delivering 150 MW dispatchable power under a 20-year PPA (2023).

Japan (Buzen, Fukuoka)
Kyushu Electric Power's 50 MW sodium-based BESS (commissioned in 2016), supporting frequency regulation and renewable integration via compact modular design and advanced SCADA control.

China (Dongying)
Single-phase EES (500 MW/1,000 MWh), uses high-density LFP cells and liquid cooling to reduce land use by 25% and offset 101k tons of coal annually.

USA (California)
Moss Landing Energy Storage Facility.Operational battery (630 MW/2,500 MWh as of 2025), storing solar surplus for California's grid.

Chile (Atacama Desert)
Operational battery storage (130 MW/5 hours, 2023), integrated with a 211 MW solar park.

Japan (Hokkaido)
17 MW/51 MWh vanadium flow battery installed on grid side (2022), centralizing renewable fluctuation management for Hokkaido Electric Power.

Australia (Collie)
Neoen's two-stage project (560 MW/~2.2 GWh total), supplying 20% of regional demand; Stage 1 (219 MW/877 MWh) operational since 2024.

Fig. 1. Global distribution of selected grid-scale electrochemical energy storage projects (2016-2025). Projects are categorized by country (distinct circular markers) and annotated with key parameters (capacity, technology type). The map highlights geographically and technologically diverse case studies, but is not exhaustive.

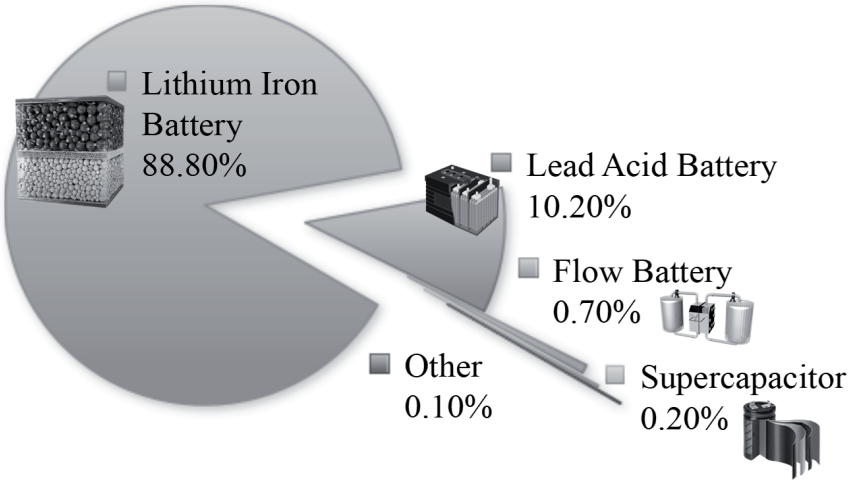

Fig. 2. Composition proportion of different types of electrochemical energy storage power stations in China.

Safety Risk Characteristics of Electrochemical Energy Storage Stations in Cold Regions

Structural Integrity and Electrolyte Leakage Mechanisms under Low-Temperature Stress

Electrochemical energy storage (EES) systems in cold climates face multiple interrelated failure pathways, as detailed in Table 1, which categorizes key issues by location, severity, and consequence [2]. One of the most critical failures originates from material embrittlement, polymers such as fluorinated rubber (FKM) seals lose elasticity below –20ºC, leading to microcracks and subsequent electrolyte leakage [10, 32]. Similarly, metals like aluminum current collectors undergo a ductile-to-brittle transition below –15ºC, reducing fracture toughness by 35% and increasing the likelihood of internal short circuits. These phenomena are often accompanied by thermal contraction mismatches, particularly at steel-polymer housing interfaces, which further compromise structural integrity and promote moisture ingress [7, 33].

Electrolyte behavior also deteriorates severely at low temperatures [34]. Conventional ethylene carbonate-based electrolytes experience a sharp viscosity increase at –40ºC, severely restricting ion mobility and fostering lithium plating [35]. As indicated in Table 1, this viscosity surge not only degrades performance but also heightens the risk of short circuits from dendrite growth [6]. Mechanical failures extend to welded connections, where uneven thermal stress causes crack propagation. Such weld joint cracking, classified as a critical hazard, introduces intermittent electrical contact, arcing, and potential fire risks [36, 37]. These risks are compounded by post-thermal runaway venting, with certain chemistries such as $LiFePO_4$ posing unexpectedly high explosion hazards in cold environments.

Mitigating these challenges demands a multifaceted approach, as demonstrated by Norway's Svalbard microgrid, where preheated enclosures maintain internal temperatures above –10ºC to minimize thermal shock [2, 4]. Advanced material solutions, including ceramic-coated separators and low-temperature polyurethane sealants, further enhance durability [38-40].

Table 1. Low-temperature failure mechanisms in Electrochemical Energy Storage (EES) system.

Issue	Location	Hazard Severity	Consequence	Reference
Polymer embrittlement	Seals/gaskets (FKM rubber)	High	Microcrack formation, electrolyte leakage, thermal runaway risk	[7, 10]
Ductile-brittle transition	Aluminum current collectors	Medium	Fracture propagation, internal short circuits, capacity fade	[7, 97]
Thermal contraction mismatch	Steel-polymer housing interfaces	High	Seal failure, moisture ingress, corrosion	[7]
Weld joint cracking	Busbar/terminal connections	Critical	Intermittent contact, arcing, fire hazard	[7, 10]
Electrolyte viscosity surge	Bulk electrolyte (EC-based)	High	Ion depletion, Li plating, dendrite penetration	[5, 41, 97]
Conductive ice formation	External surfaces post-leakage	Critical	Ground faults, system shutdown	[5, 11, 41, 98]

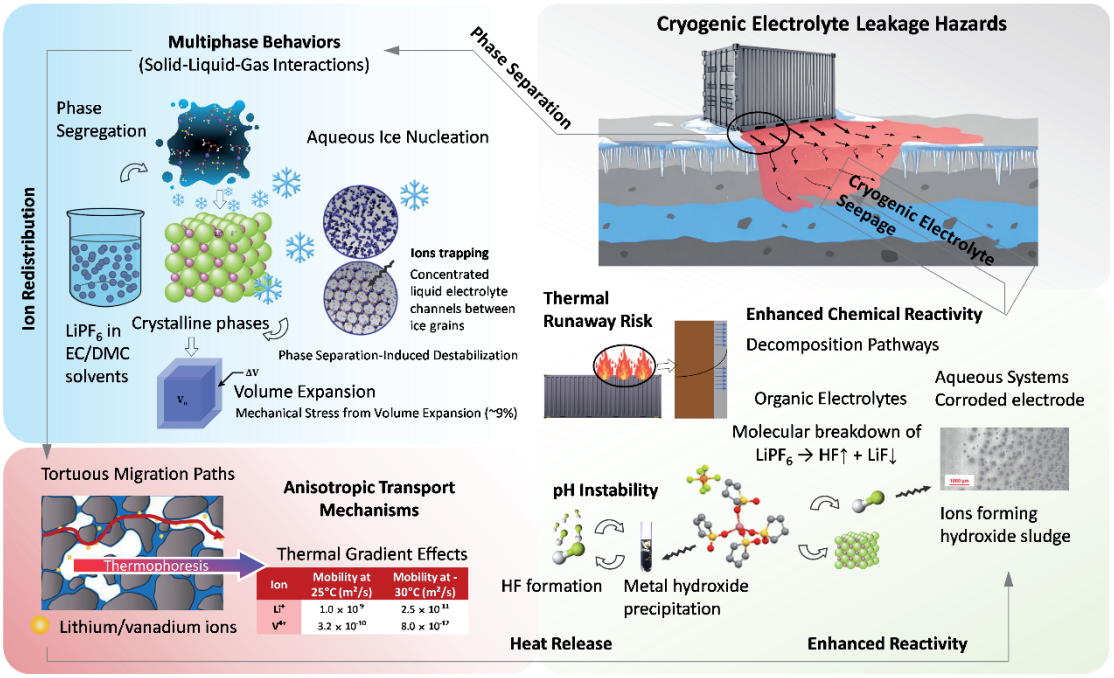

Fig. 3. Multiscale hazards of cryogenic electrolyte leakage: phase instability, enhanced reactivity, and anisotropic transport.

Collectively, these measures underscore the necessity of adaptive design and operational strategies to ensure EES reliability in extreme cold [2, 5, 38].

Multiphase Environmental Hazards from Leakage in Cryogenic Conditions

Under cryogenic conditions, leaked electrolytes exhibit complex multiphase behaviors that exacerbate environmental and safety risks (Fig. 3) [21]. In Li-ion batteries, organic carbonate-based electrolytes undergo freezing below –20ºC, forming crystalline phases that destabilize solvation structures and accelerate salt precipitation [41], while aqueous electrolytes experience ice nucleation, leading to solute concentration polarization and localized corrosion hotspots [11]. The coexistence of solid (ice/crystals), liquid (supercooled electrolyte), and gaseous phases (evaporated solvents) creates thermodynamically unstable interfaces, promoting dendritic crystallization and micro-fractures in containment materials [2]. Such phase heterogeneity further disrupts mass transport, as seen in the Ostwald ripening of Li salts or the segregation of vanadium ions in frozen aqueous systems, amplifying leakage-driven degradation. These phenomena are compounded by the volume expansion of freezing electrolytes (e.g., ~9% for water), which mechanically stresses battery housings and adjacent infrastructure [27].

Low temperatures significantly alter the chemical reactivity of leaked electrolytes, often intensifying hazardous side reactions [15]. In lithium-ion batteries, the decomposition of organic carbonate solvents (ethylene carbonate, dimethyl carbonate, ethyl methyl carbonate) becomes more exothermic at subzero temperatures due to slowed kinetics of passivation layer formation, leading to uncontrolled heat release and potential thermal runaway [41]. Concurrently, the hydrolysis of lithium salts such as $LiPF_6$ generates corrosive byproducts, including hydrogen fluoride gas, lithium fluoride precipitates, and phosphorus oxyfluorides, which compromise structural materials and pose inhalation risks [23]. Similarly, aqueous electrolytes in flow batteries exhibit accelerated corrosion of electrodes and membranes at cryogenic conditions, driven by the increased solubility of reactive oxygen species and the destabilization of redox-active ions like vanadium or zinc. These reactions are further exacerbated by the reduced efficiency of buffer systems at low temperatures, resulting in pH swings that promote the precipitation of metal hydroxides or oxides. Such temperature-dependent reactivity not only escalates immediate safety hazards but also contributes to long-term environmental persistence of contaminants [2, 11].

Electrolyte leakage exhibits unique transport behaviors dominated by thermally driven phase transitions and interfacial phenomena [42]. The diffusion of lithium salts ($LiPF_6$, LiTFSI, LiFSI) and redox-active ions (vanadium, zinc, iron) becomes highly anisotropic as freezing temperatures induce salt precipitation and ice nucleation, creating tortuous migration pathways through partially frozen matrices [11]. Ice formation restructures transport mechanisms through solute exclusion effects that concentrate electrolytes at grain boundaries, generating high-conductivity brine channels beneath ice layers [27]. These microstructural features enable accelerated contaminant migration along thermal gradients while simultaneously blocking bulk diffusion, leading to complex spatiotemporal distribution patterns.

Molecular dynamics simulations reveal that subzero temperatures reduce ionic mobility but enhance directional migration forces, resulting in preferential flow paths that exacerbate localized corrosion and environmental contamination [2, 41]. Such cryogenic-specific transport phenomena necessitate advanced modeling approaches that account for phase separation and interfacial electrochemistry in containment system design.

Transport Mechanism of Electrolyte at Cryogenic Conditions

The Temperature-Dependent Behavior of Electrolytes across Macropores and Micropores

Understanding of temperature effects in liquid battery electrolytes, spanning macroscopic transport to microscopic processes, is extensively documented. This is especially documented for $LiPF_6$/carbonate systems [43, 44]. However, there remain significant knowledge gaps, particularly in areas such as interfacial transport involving the solid electrolyte interphase (SEI), multicomponent cross-drag effects, and unified transport models that span different chemistries and temperature extremes.

Temperature-Dependent Electrolyte Transport in Macropores and Micropores

Ionic conductivity and ion/solvent diffusion coefficients universally decrease with decreasing temperature, typically following Arrhenius or compensated Arrhenius scaling, particularly when accounting for temperature-dependent dielectric effects [44, 45]. At the microscopic level, most liquid electrolytes exhibit only modest temperature-driven changes in Li^+ solvation structure. Spectroscopic studies reveal a slight shift toward contact-ion pairs (CIP) at higher temperatures and solvent-separated ion pairs (SSIP) at lower temperatures, especially in carbonate-based systems [43]. Nuclear magnetic resonance (NMR) and molecular dynamics (MD) analyses confirm minimal temperature-induced changes in ion-pairing statistics, indicating that viscosity and solvation effects dominate transport behavior across temperature regimes rather than ion aggregation [43, 44, 46]. This is particularly evident in $LiPF_6$/carbonate systems where viscosity governs low-temperature ionic mobility, with no significant aggregation observed down to -20°C [44]. Notably, Li^+ transference numbers remain largely temperature-invariant, though certain reference frames may exhibit non-monotonic dependencies [35]. These transport characteristics correlate strongly with temperature-induced changes in solvation equilibrium free energy [43], demonstrating interconnected macro-micro relationships where macroscopic transport trends emerge directly from molecular-scale interactions.

Advanced Transport Coefficient Sets

Transport in concentrated or multicomponent electrolytes remains underexplored. Only one study has provided a comprehensive set of Stefan–Maxwell (Onsager) coefficients, such as temperature-dependent cross-drag coefficients ($\Lambda_{ij}(T)$) and Soret/Seebeck coefficients. Hanke et al. [45] verified that thermally driven polarization can rival ohmic losses under certain cell conditions. Other works typically focus on bulk metrics, leaving cross-effects underexplored. Modern efforts integrating simulations and experiments have shed light on the sensitivity of transference numbers and cross-coefficients to the choice of reference frame. These insights begin to resolve prior inconsistencies in results [47].

Interfacial and Operando Transport Studies

There is minimal direct characterization of temperature-dependent SEI/interphase transport properties, as such contributions are often subsumed into total cell impedance measurements or overlooked. Early operando imaging techniques, including Raman spectroscopy and MRI, have begun to isolate temperature-driven concentration gradients during operation, providing valuable insights into these processes. Recent advances in gradient-resolved Raman [48] and MRI/NMR [49] imaging demonstrate real-time tracking of temperature-dependent changes in local diffusivity, concentration polarization, and the onset of lithium filamentation under thermal gradients.

Chemistry and Temperature Coverage

The majority of studies focus on $LiPF_6$/carbonate systems, with secondary coverage of polymer electrolytes [47, 50, 51] and ether/glyme systems [43, 48, 52]. There remains sparse data for aqueous systems, ionic liquids (ILs), and solid-state electrolytes. Comparative studies of alternate cations and salts (e.g., Na^+, K^+, TFSI, FSI) indicate expected trends in solvation and diffusion, but lack extensive temperature-dependent data [52, 53]. Most research is confined to the range of –20ºC to +60ºC, with some studies extending to –60ºC or +90ºC for extreme cases involving glassy/polymer electrolytes or liquid systems [43, 44, 51]. However, detailed investigations focusing on interfacial dynamics or non-liquid-state phenomena at these limits remain limited.

Models, Scaling Laws, and Outstanding Challenges

Recent advances in modeling show that non-Arrhenius conductivity in bulk liquids can be accurately described using compensated Arrhenius scaling. This approach captures temperature-dependent changes in the solvent's dielectric properties without invoking multiple mechanistic barriers, simplifying the analysis

of typical organic liquid electrolytes [54]. Cutting-edge hybrid simulations (e.g., MD with continuum models) and advanced spectroscopies are beginning to resolve full transport coefficient sets, including cross-coupling effects and thermo-diffusion phenomena, while linking them to thermodynamic and kinetic descriptors [43, 45, 47]. However, experimental validation of these frameworks is still in its early stages. No robust framework currently exists to separate and quantify SEI or interfacial conductivity activation energies and their scaling with temperature. This remains critical for next-generation modeling and optimizing electrochemical performance under extreme temperature conditions. Few studies systematically investigate multicomponent friction, cross-drag, and temperature-dependent thermodiffusion parameters [45]. There remains fragmentation in experimental and theoretical integration, particularly for non-traditional electrolyte systems like ionic liquids, water-in-salt electrolytes, and solids, as well as at temperature extremes.

Experimental Studies on Electrolyte Transport under Frozen or Freeze–Thaw Conditions

Experimental and modeling advances have significantly elucidated the complex behavior of solute transport in frozen soils, integrating direct measurements with physically based numerical frameworks. Controlled laboratory studies using soil columns [55-57] provide fundamental insights into ion migration mechanisms under various freezing regimes. Investigations expanded to cyclic freeze-thaw scenarios, documenting complete mass balance and redistribution profiles for Na_2SO_4 in silt [58], while quantifying NaCl and water movement in sand under constant freezing rates [59]. Field-based observations further demonstrate environmental relevance, with tracking multi-ion accumulation (Cl^-, Na^+, Mg^{2+}, Ca^{2+}) during seasonal transitions in agricultural systems and employing KBr tracers to monitor conductivity changes through freeze-thaw cycles [60, 61]. Advanced methodologies like time-domain reflectometry enable precise tracking of coupled water-electrolyte movement [62], while studies such as systematically compare diverse electrolytes (Na_2SO_4, KCl, $CaCl_2$, NaCl, $MgCl_2$) in hydrate-bearing sediments [55], revealing salt-specific phase transition behaviors that govern ion mobility in frozen matrices.

Complementing empirical findings, physically-based numerical models [63-69] simulate the coupled thermo-hydro-chemical processes governing cryogenic solute transport. Early modeling by Panday and Corapcioglu [70] established fundamental frameworks for salt rejection and redistribution during freezing, incorporating capillary and Clapeyron effects. Subsequent 1D formulations [63, 67] integrate advection-dispersion mechanisms with coupled driving potentials (matric, osmotic, vapor), enabling prediction of precipitation zones [67] and ice lens formation under saline conditions. Notably, recent multidimensional advances include Mohammed's [66] 2D framework for permafrost-affected groundwater contaminant transport and Huang's [64] sophisticated finite-element model that fully couples water/heat/solute transport with soil deformation and sorption processes. Field-scale predictive capabilities are enhanced through landscape solute connectivity models under degrading permafrost [71] and seasonal freeze-thaw scenarios [65, 72]. Crucially, iterative model-experiment validation [55, 67] ensures predictive reliability, evidenced by close matches between simulated and measured salt profiles in unsaturated columns, Na_2SO_4 mass balance under cyclic freezing [58], and ion flux densities in phase-transition systems [55].

Microscale mechanisms underpinning these dynamics involve complex interfacial processes where premelting enables solute migration through nanoscale unfrozen films [73], and solute rejection at advancing ice fronts leads to brine entrapment and channelization [75, 76]. Research by Zhang et al. [9] reveals how alternating ice and salt crystallization generates deformation through supersaturation and pressure buildup, particularly consequential in sulfate-rich systems. Fundamental investigations of clay-water-salt interactions [76] and hydrate dissociation constraints [55] further establish the physicochemical basis for ion mobility. These microscale phenomena directly manifest in macroscale hydro-mechanical coupling, where frost heave and soil deformation interact dynamically with solute redistribution, as quantified through laboratory deformation tracking and integrated into comprehensive numerical frameworks [64]. The collective advances across experimental, theoretical, and computational domains now enable predictive understanding of electrolyte behavior in frozen terrestrial systems – from pore-scale phase transitions to landscape-scale contaminant pathways in warming permafrost regions.

Coupled Water and Heat Transfer Processes in Cold Regions

In cold regions, the convective-dispersive equation of solute transport is an important tool for understanding how solutes move through the frozen soil matrix. This equation is based on the principles of mass balance and considers both convective transport (driven by fluid flow) and dispersive transport (driven by concentration gradients). The general form of the convective-dispersive equation in frozen soils can be expressed as follows:

$$\frac{\partial(\theta c)}{\partial t} = \nabla \cdot (\theta D \nabla c) - \nabla \cdot (qc) + \phi \quad (1)$$

Where θ is volumetric soil water content, c is solute concentration in soil solution, D is dispersion coefficient, q is liquid water flux, ϕ is a sink term for solute degradation and extraction by roots. Water transport

during freezing/thawing combines liquid and phase-change dynamics and can be expressed as follows:

$$\frac{\partial \theta_l}{\partial t} + \frac{\rho_i}{\rho_l}\frac{\partial \theta_i}{\partial t} = \nabla \cdot [K(\theta_l)\nabla(\psi + z)] + S \quad (2)$$

Where θ_l is liquid water content, $K(\theta_l)$ is unsaturated soil hydraulic conductivity, ψ is soil matric potential, S is a source/sink term for water flow. Thermal dynamics drive phase transitions:

$$C_s \frac{\partial T}{\partial t} + L_f \rho_i \frac{\partial \theta_i}{\partial t} = \nabla \cdot (\kappa \nabla T) - \rho_l C_l \nabla \cdot (qT) \quad (3)$$

Where C_s is heat capacity of soil, T is soil temperature, L_f is latent heat of fusion, θ_i is ice content within soil, ρ_i is density of ice, κ is soil heat conductivity, ρ_l and C_l are density and heat capacity of liquid water, respectively.

Physically-based modeling of coupled hydrothermal processes in frozen soils employs several established frameworks. The Simultaneous Heat and Water (SHAW) model dynamically simulates liquid, solid, and gaseous water phases through freezing-point water potential equations, eliminating reliance on a fixed 0ºC threshold [77, 78]. It has been extensively applied to quantify heat-water-solute interactions with vegetation/snow cover [79, 80], permafrost thermal regimes [81], and groundwater table effects [82]. In contrast, the CoupModel [83] integrates conduction and vapor convection while explicitly accounting for ice-induced moisture migration dynamics, enabling simulations of hydrothermal fluxes [8, 84], water-heat-salt coupling [85], and organic matter impacts on permafrost [86]. Its parameter uncertainty is minimized through automated GLUE-MCMC calibration [87]. The Hydrus-1D model excels in simulating water/vapor/heat movement under nonfreezing conditions, with enhanced freezing modules incorporating hydraulic conductivity blocking effects [88], though it omits frost heave mechanics.

Critical distinctions exist between these approaches: SHAW utilizes the Clapeyron equation and de Vries thermal parameterization but neglects bypass flow, making it particularly effective for salt transport modeling [90]. Conversely, CoupModel's threshold-based thermal conductivity and accommodation of bypass flow improve accuracy in freeze-thaw hydrothermal cycling and cold-region ecological processes [81]. Alternative methodologies include enthalpy-based formulations [90] that replace temperature with volumetric enthalpy in energy balance equations to circumvent phase-change instability, significantly enhancing computational efficiency [91]. Engineering-oriented finite-element platforms like COMSOL Multiphysics and ANSYS resolve coupled differential equations for saturated/unsaturated zones [12], enabling detailed analysis of vapor transfer mechanisms [92] and phase-change dynamics [93], albeit with high parametric demands that limit regional scalability.

Ongoing model advancements address complex interfacial behaviors, including nonequilibrium ice-water interfaces [94] and coupled liquid-vapor-air fluxes [95], while land-surface integrations (e.g., HydroSiB2 [90]) and seasonal process modules [96] continue to refine representations of energy-mass-momentum coupling in permafrost environments. These developments collectively advance predictive capabilities for frozen soil hydro-thermal dynamics across scales, despite persistent challenges in balancing physical fidelity with computational tractability.

Conclusions

Addressing electrolyte leakage in cold-region energy storage is vital for sustainable infrastructure and environmental safety. This review synthesizes cryogenic failure mechanisms: subzero conditions induce electrolyte phase separation (e.g., $LiPF_6$ precipitation, vanadium hydrate crystallization) and material embrittlement, exacerbating containment breaches. Freeze-thaw dynamics dominate the anisotropic transport of leaked electrolytes. Specifically, ice formation restricts vertical leaching while redirecting contaminants laterally through unfrozen brine channels and frost-heaved fractures. These transport processes are further amplified by thermal gradients via solute exclusion and Soret effects. Cryogenic reactivity intensifies hazards (accelerated HF release, heightened vanadium oxidation), destabilizing soils. Physically based models (SHAW, CoupModel, Hydrus-1D) simulate thermo-hydro-chemical coupling but lack resolution for interfacial electrochemistry at ice boundaries and multicomponent cross-drag in frozen media. Future work would prioritize four interconnected research vectors to advance predictive capabilities and mitigation strategies:

(1) Interfacial Electrochemistry Quantification: Advanced operando cryogenic characterization techniques are needed to resolve charge transfer mechanisms across solid electrolyte interphases (SEI) and ice-electrolyte interfaces.

(2) Multicomponent Transport Validation: Experimental-computational co-validation of cross-drag coefficients and Soret parameters for complex electrolytes under freeze-thaw cycling, particularly in heterogeneous frozen soils.

(3) Multiscale Model Integration: Development of unified computational frameworks integrating molecular dynamics simulations of premelting films with pore-scale phase-field models of ice lens formation and field-scale continuum models predicting contaminant transport in permafrost terrains.

(4) Extreme Environment Material Design: Machine learning-driven discovery of electrolyte formulations and sealants evaluated under cryogenic thermal cycling with simultaneous mechanical stress.

Acknowledgements

This study was funded by the Science and Technology Project of PowerChina Huadong Engineering Corporation Limited (KY2023-XNY-02-26, 24H0633).

Conflict of Interest

The authors declare no conflict of interest.

References

1. ABBAS Q., MIRZAEIAN M., HUNT M.R.C., HALL P., RAZA R. Current State and Future Prospects for Electrochemical Energy Storage and Conversion Systems. Energies. **13** (21), 5847, **2020**.
2. CHEN M., ZHANG Y., XING G., CHOU S., TANG Y. Electrochemical energy storage devices working in extreme conditions. Energy & Environmental Science. **14** (6), 3323, **2021**.
3. KANG D., ZHANG W., LIU J., MIAO Y., LIU W., ZENG B., LI Z., CHEN Z., FANG R., XI B. Development of electrochemical energy storage and application in power grid. In 2022 IEEE 2nd International Conference on Power, Electronics and Computer Applications (ICPECA). IEEE, Shenyang, China, pp. 1166-1171, **2022**.
4. MÜLLER C.M., SAND S.E. A study of microgrids in Norway: Mapping the motivations, benefits, challenges and prerequisites required for extensive use of microgrids in Norway. Bacherol Thesis, Norwegian University of Science and Technology, **2021**.
5. AHOUTOU Y., ILINCA A., ISSA M. Electrochemical Cells and Storage Technologies to Increase Renewable Energy Share in Cold Climate Conditions – A Critical Assessment. Energies. **15** (4), 1579, **2022**.
6. HOLOUBEK J., LIU H., WU Z., YIN Y., XING X., CAI G., YU S., ZHOU H., PASCAL T.A., CHEN Z., LIU P. Tailoring Electrolyte Solvation for Li Metal Batteries Cycled at Ultra-Low Temperature. Nature Energy. **2021**, **2021**.
7. MADDIPATLA S., KONG L., PECHT M. Electrolyte Leakage in Cylindrical Lithium-Ion Batteries Subjected to Temperature Cycling. Energies. **17** (7), 1533, **2024**.
8. WU M., WU J., TAN X., HUANG J., JANSSON P., ZHANG W., STRATEGISKA F.S., PROFILOMRÅDEN O.A.S.F., MERGE M.T.R.A., LUND U., BECC B.A.E.S., PROFILE A.A.O.S., STRATEGIC R.A.S., LUNDS U. Simulation of dynamical interactions between soil freezing/thawing and salinization for improving water management in cold/arid agricultural region. Geoderma. **338**, 325, **2019**.
9. ZHANG J., LAI Y., ZHAO Y., LI S. Study on the mechanism of crystallization deformation of sulfate saline soil during the unidirectional freezing process. Permafrost and Periglacial Processes. **32** (1), 102, **2021**.
10. JAUMAUX P., WU J., SHANMUKARAJ D., WANG Y., ZHOU D., SUN B., KANG F., LI B., ARMAND M., WANG G. Non-Flammable Liquid and Quasi-Solid Electrolytes toward Highly-Safe Alkali Metal-Based Batteries. Advanced Functional Materials. **31** (10), **2021**.
11. WANG Y., WEI H., LI Z., ZHANG X., WEI Z., SUN K., LI H. Optimization Strategies of Electrolytes for Low-Temperature Aqueous Batteries. The Chemical Record. **22** (10), e202200132, **2022**.
12. KURYLYK B.L., MCKENZIE J.M., MACQUARRIE K.T.B., VOSS C.I. Analytical solutions for benchmarking cold regions subsurface water flow and energy transport models: One-dimensional soil thaw with conduction and advection. Advances in Water Resources. **70**, 172, **2014**.
13. CHEN Y., KANG Y., ZHAO Y., WANG L., LIU J., LI Y., LIANG Z., HE X., LI X., TAVAJOHI N., LI B. A review of lithium-ion battery safety concerns: The issues, strategies, and testing standards. Journal of Energy Chemistry. **59**, 83, **2021**.
14. RAJESHWAR K., BALTRUSCHAT H., SUN Y.K. Electrochemical Energy Conversion: Past, Present, and Future. Chemphyschem. **15** (10), 1903, **2014**.
15. CHEN T., JIN Y., LV H., YANG A., LIU M., CHEN B., XIE Y., CHEN Q. Applications of Lithium-Ion Batteries in Grid-Scale Energy Storage Systems. Transactions of Tianjin University. **26** (3), 208, **2020**.
16. CRABTREE G., KÓCS E., TRAHEY L. The energy-storage frontier: Lithium-ion batteries and beyond. Mrs Bulletin. **40** (12), 1067, **2015**.
17. LIU Z., LIU J., ZHAO S., XUN S., BYARUHANGA P., CHEN S., TANG Y., ZHU T., CHEN H. Low-cost iron trichloride cathode for all-solid-state lithium-ion batteries. Nature Sustainability. **7** (11), 1492, **2024**.
18. MURALIDHARAN N., ESSEHLI R., HERMANN R.P., PAREJIYA A., AMIN R., BAI Y., DU Z., BELHAROUAK I. $LiNi_xFe_yAl_zO_2$, a new cobalt-free layered cathode material for advanced Li-ion batteries. Journal of Power Sources. **471** (1), 228389, **2020**.
19. KEBEDE A.A., KALOGIANNIS T., Van MIERLO J., BERECIBAR M. A comprehensive review of stationary energy storage devices for large scale renewable energy sources grid integration. Renewable & Sustainable Energy Reviews. **159**, 112213, **2022**.
20. XU Y., PEI J., CUI L., LIU P., MA T. The Levelized Cost of Storage of Electrochemical Energy Storage Technologies in China. Frontiers in Energy Research. **10**, 873800, **2022**.
21. SUN J., LIU C., SONG X., ZHANG J., LIU Y., LIANG L., JIANG R., YUAN C. Electrochemical energy storage devices under particular service environments: Achievements, challenges, and perspective. Applied Physics Reviews. **9** (3), 31301, **2022**.
22. RAGUPATHY P., BHAT S.D., KALAISELVI N. Electrochemical energy storage and conversion: An overview. Wiley Interdisciplinary Reviews-Energy and Environment. **12** (2), e464, **2023**.
23. XIA L., YU L., HU D., CHEN G.Z. Electrolytes for electrochemical energy storage. Materials Chemistry Frontiers. **1** (4), 584, **2017**.
24. ZHANG C., ZHANG L., YU G. Eutectic Electrolytes as a Promising Platform for Next-Generation Electrochemical Energy Storage. Accounts of Chemical Research. **53** (8), 1648, **2020**.
25. LAN S., YU C., YU J., ZHANG X., LIU Y., XIE Y., WANG J., QIU J. Recent Advances in Low-Temperature Liquid Electrolyte for Supercapacitors. Small. **21** (28), e2309286, **2024**.
26. KHOR C.K., BLACKSTONE C.C., IGNASZAK A. An Insight into Synthesis of the Antifreeze Alkaline Hydrogel Electrolyte: Fine-Tuning Chemistries for Efficient Ion Transport. ChemElectroChem. **10** (16), e202300113, **2023**.

27. WANG C., LI K., CAI H., WU Y., LIN Z., LI S. Study of Supercooling Phenomena in Soil-Water Systems Based on Nucleation Theory: Quantifying Supercooling Degree. Water Resources Research. **59** (11), e2023WR035935, **2023**.
28. HU G., ZHAO L., ZHU X., WU X., WU T., LI R., XIE C., HAO J. Review of algorithms and parameterizations to determine unfrozen water content in frozen soil. Geoderma. **368**, 114277, **2020**.
29. LIU B., HE L., LI C., HAN Y., SUN Y., HAN Q., ZENG J. Study on electrical properties of saline frozen soil and influence mechanism of unfrozen water content. Cold Regions Science and Technology. **220**, 104146, **2024**.
30. YANG X., HU J., MA R., SUN Z. Integrated Hydrologic Modelling of Groundwater-Surface Water Interactions in Cold Regions. Frontiers in Earth Science. **9**, 721009, **2021**.
31. ZHANG J., LAI Y., ZHANG M., YOU Z., LI S., BAI R. Study on the coupling mechanism of water-heat-vapor-salt-mechanics in unsaturated freezing sulfate saline soil. Computers and Geotechnics. **169**, 106232, **2024**.
32. SO J.I., LEE C.S., JUNG J.Y., LEE J., CHOI J.K., SHIM S.E., QIAN Y. Optimization and Characterization of the F-LSR Manufacturing Process Using Quaternary Ammonium Silanolate as an Initiator for Synthesizing Fluorosilicone. Polymers. **14** (24), 5502, **2022**.
33. SHIMIZU T., KISHI R., KOBASHI K., MORIMOTO T., OKAZAKI T., YAMADA T., HATA K. Improved thermal stability of silicone rubber nanocomposites with low filler content, achieved by well-dispersed carbon nanotubes. Composites Communications. **22**, 100482, **2020**.
34. YANG Y., YANG W., YANG H., ZHOU H. Electrolyte design principles for low-temperature lithium-ion batteries. eScience. **3** (6), 100170, **2023**.
35. HICKSON D.T., IM J., HALAT D.M., KARVAT A., REIMER J.A., BALSARA N.P. Low-Temperature Characterization of a Nonaqueous Liquid Electrolyte for Lithium Batteries. Journal of the Electrochemical Society. **171** (3), 030514, **2024**.
36. RINNE J., SEFFER O., NOTHDURFT S., HERMSDORF J., KAIERLE S., OVERMEYER L. Investigations on the weld metal composition and associated weld metal cracking in laser beam welded steel copper dissimilar joints. Journal of Materials Processing Technology. **296**, 117178, **2021**.
37. ZHAO K., CUI Q., WANG B., YANG F. Probabilistic analysis of crack tip mechanical properties in welded joints for nuclear structures. Structures. **48**, 125, **2023**.
38. MA T., PAN Z., MIAO L., CHEN C., HAN M., SHANG Z., CHEN J. Porphyrin-Based Symmetric Redox-Flow Batteries towards Cold-Climate Energy Storage. Angewandte Chemie International Edition. **57** (12), 3158, **2018**.
39. YANG J., SHANG J., LIU Q., YANG X., TAN Y., ZHAO Y., LIU C., TANG Y. Variant-Localized High-Concentration Electrolyte without Phase Separation for Low-Temperature Batteries. Angewandte Chemie International Edition. **63** (33), e202406182, **2024**.
40. ZHENG S., KHAN N., WORKU B.E., WANG B. Review and prospect on low-temperature lithium-sulfur battery. Chemical Engineering Journal. **484**, 149610, **2024**.
41. SUN Y., LIU B., LIU L., YAN X. Ions Transport in Electrochemical Energy Storage Devices at Low Temperatures. Advanced Functional Materials. **32** (15), 2109568, **2022**.
42. CHEONG D.S., HEO E.S., HONG J., YOO S., JEON Y., JEONG J., LEE M.H., SONG H.K. Freeze-Vulnerable Plastic Crystal to Cryogenic Liquid Electrolyte for Lithium Batteries by Deep Freezing-Point Depression. Small. **20** (47), e2404722, **2024**.
43. LAI J., GUO Y., LAI H.E., OSPINA-ACEVEDO F.A., TIAN W., KUAI D., CHEN D., BALBUENA P.B., SHI F. Linking Solvation Equilibrium Thermodynamics to Electrolyte Transport Kinetics for Lithium Batteries. Journal of the American Chemical Society. **147** (17), 14348, **2025**.
44. RINGSBY A.J., FONG K.D., SELF J., BERGSTROM H.K., MCCLOSKEY B.D., PERSSON K.A. Transport Phenomena in Low Temperature Lithium-Ion Battery Electrolytes. Journal of the Electrochemical Society. **168** (8), 080501, **2021**.
45. HANKE F., MODROW N., AKKERMANS R.L.C., KOROTKIN I., MOCANU F.C., NEUFELD V.A., VEIT M. Multi-Scale Electrolyte Transport Simulations for Lithium Ion Batteries. Journal of the Electrochemical Society. **167** (1), 13522, **2020**.
46. BERHAUT C.L., LEMORDANT D., PORION P., TIMPERMAN L., SCHMIDT G., ANOUTI M. Ionic association analysis of LiTDI, LiFSI and $LiPF_6$ in EC/DMC for better Li-ion battery performances. RSC Advances. **9** (8), 4599, **2019**.
47. SHAO Y., GUDLA H., MINDEMARK J., BRANDELL D., ZHANG C. Ion Transport in Polymer Electrolytes: Building New Bridges between Experiment and Molecular Simulation. Accounts of Chemical Research. **57** (8), 1123, **2024**.
48. OLBRICH L.F., JAGGER B., IHLI J., PASTA M. Operando Raman Gradient Analysis for Temperature-Dependent Electrolyte Characterization. ACS Energy Letters. **9** (7), 3636, **2024**.
49. KRACHKOVSKIY S.A., BAZAK J.D., WERHUN P., BALCOM B.J., HALALAY I.C., GOWARD G.R. Visualization of Steady-State Ionic Concentration Profiles Formed in Electrolytes during Li-Ion Battery Operation and Determination of Mass-Transport Properties by in Situ Magnetic Resonance Imaging. Journal of the American Chemical Society. **138** (25), 7992, **2016**.
50. TIMACHOVA K., CHINTAPALLI M., OLSON K.R., MECHAM S.J., DESIMONE J.M., BALSARA N.P. Mechanism of ion transport in perfluoropolyether electrolytes with a lithium salt. Soft Matter. **13** (32), 5389, **2017**.
51. TSAMOPOULOS A.J., WANG Z.G. Ion Conductivity in Salt-Doped Polymers: Combined Effects of Temperature and Salt Concentration. ACS Macro Letters. **13** (3), 322, **2024**.
52. ARDHRA S., PRAKASH P., SIVA D.R., VENKATNATHAN A. Effect of Concentration and Temperature on the Structure and Ion Transport in Diglyme-Based Sodium-Ion Electrolyte. Journal of Physical Chemistry B. **126** (10), 2119, **2022**.
53. KARATRANTOS A.V., MIDDENDORF M., NOSOV D.R., CAI Q., WESTERMANN S., HOFFMANN K., NURNBERG P., SHAPLOV A.S., SCHONHOFF M. Diffusion and structure of propylene carbonate-metal salt electrolyte solutions for post-lithium-ion batteries: From experiment to simulation. Journal of Chemical Physics. **161** (5), 054502, **2024**.
54. SHCHERBAKOV V.V., ARTEMKINA Y.M., AKIMOVA I.A., ARTEMKINA I.M. Dielectric Characteristics, Electrical Conductivity and Solvation of Ions

in Electrolyte Solutions. Materials. **14** (19), 5617, **2021**.
55. CHUVILIN E., EKIMOVA V., DAVLETSHINA D., BUKHANOV B., KRIVOKHAT E., SHILENKOV V. Migration of Salt Ions in Frozen Hydrate-Saturated Sediments: Temperature and Chemistry Constraints. Geosciences. **12** (7), 276, **2022**.
56. GRIGORIEV B.V., YANBIKOVA Y.F. Investigation of salt migration in the ground saturated with a chloride-sulphate sodium-magnesium solution in freezing-thawing cycles. MATEC Web of Conferences. **265**, 06008, **2019**.
57. KROGSTAD K., GHARASOO M., JENSEN G., HUG L.A., RUDOLPH D., Van CAPPELLEN P., REZANEZHAD F. Nitrogen Leaching From Agricultural Soils Under Imposed Freeze-Thaw Cycles: A Column Study With and Without Fertilizer Amendment. Frontiers in Environmental Science. **10**, 915329, **2022**.
58. BING H., HE P., ZHANG Y. Cyclic freeze–thaw as a mechanism for water and salt migration in soil. Environmental Earth Sciences. **74** (1), 675, **2015**.
59. CHEN M., LIU R., DONG Z. Effect of Different Chloride Salts on the Transport of Water, Heat, and Solutes in Sandy Soil under Freezing Conditions. Journal of Cold Regions Engineering. **37** (3), 04023013, **2023**.
60. LIU Y., WU J., ZHAO H., LI C., MAO J., ZHANG R., LIU J., ZHAO Q. Ions Transport in Seasonal Frozen Farmland Soil and Its Effect on Soil Salinization Chemical Properties. Agronomy-Basel. **13** (3), 660, **2023**.
61. VAIPHEI S.P., KURAKALVA R.M. Hydrochemical characteristics and nitrate health risk assessment of groundwater through seasonal variations from an intensive agricultural region of upper Krishna River basin, Telangana, India. Ecotoxicology and Environmental Safety. **213**, 112073, **2021**.
62. WAN H., LI X., LUO Y., SHI D., GONG T., AN A.K., SHAO S. Early monitoring of pore wetting in membrane distillation using ultrasonic time-domain reflectometry (UTDR). Water Research. **240**, 120081, **2023**.
63. BAO D., ZHANG Z., YUE Z., ZHANG A., LIU G. Study on the water–salt migration law of salinized frozen soil based on the capillary model. Frontiers in Earth Science. **12**, 1367771, **2024**.
64. HUANG X., RUDOLPH D.L. Numerical Study of Coupled Water and Vapor Flow, Heat Transfer, and Solute Transport in Variably-Saturated Deformable Soil During Freeze-Thaw Cycles. Water Resources Research. **59** (10), e2022WR032146, **2023**.
65. KELLENERS T.J. Coupled water flow, heat transport, and solute transport in a seasonally frozen rangeland soil. Soil Science Society of America Journal. **84** (2), 399, **2020**.
66. MOHAMMED A.A., BENSE V.F., KURYLYK B.L., JAMIESON R.C., JOHNSTON L.H., JACKSON A.J. Modeling Reactive Solute Transport in Permafrost-Affected Groundwater Systems. Water Resources Research. **57** (7), e2020WR028771, **2021**.
67. ZHANG X., WANG Q., WANG G., WANG W., CHEN H., ZHANG Z. A Study on the Coupled Model of Hydrothermal-Salt for Saturated Freezing Salinized Soil. Mathematical Problems in Engineering. **2017** (1), 4918461, **2017**.
68. SUN L., TANG X., ABOAYANAH K.R., ZHAO Q., LIU Q., GRASSELLI G. A coupled cryogenic thermo-hydro-mechanical model for frozen medium: Theory and implementation in FDEM. Journal of Rock Mechanics and Geotechnical Engineering. **16** (11), 4335, **2024**.
69. VIDAL R., SAALTINK M.W. A novel method for decoupling thermo-hydraulic processes from chemical reactions to understand the effect of heat on chemical reaction. Geothermics. **126**, 103203, **2025**.
70. PANDAY S., CORAPCIOGLU M.Y. Solute rejection in freezing soils. Water Resources Research. **27** (1), 99, **1991**.
71. FRAMPTON A., DESTOUNI G. Impact of degrading permafrost on subsurface solute transport pathways and travel times. Water Resources Research. **51** (9), 7680, **2015**.
72. WANG K., WU M., ZHANG R. Water and Solute Fluxes in Soils Undergoing Freezing and Thawing. Soil Science. **181** (5), 193, **2016**.
73. WAN X., PEI W., LU J., ZHANG X., YAN Z., PIRHADI N. Prediction of the unfrozen water content in soils based on premelting theory. Journal of Hydrology. **608**, 127505, **2022**.
74. RASMUSSEN A., JANNAT M., WANG H. Fundamentals of freeze desalination: Critical review of ion inclusion and rejection studies from molecular dynamics perspective. Desalination. **573**, 117216, **2024**.
75. SHISHINY A.M., KADER A.M., AHMED S., RASHAD M.I. An investigation of a proposed freezing desalination system integrating sweating effect and a Centrifugal-Based brine rejection technique. Separation and Purification Technology, **353**, 128390, **2025**.
76. LIU J., YANG P., YANG Z.J. Water and salt migration mechanisms of saturated chloride clay during freeze-thaw in an open system. Cold Regions Science and Technology. **186**, 103277, **2021**.
77. TAN X., WU J., WU M., HUANG J., TAN B., LI L. Effects of ice cover on soil water, heat, and solute movement: An experimental study. Geoderma. **403**, 115209, **2021**.
78. HU G., ZHAO L., LI R., PARK H., WU X., SU Y., GUGGENBERGER G., WU T., ZOU D., ZHU X., ZHANG W., WU Y., HAO J. Water and heat coupling processes and its simulation in frozen soils: Current status and future research directions. Catena. **222**, 106844, **2023**.
79. HE H., FLERCHINGER G.N., KOJIMA Y., HE D., HARDEGREE S.P., DYCK M.F., HORTON R., WU Q., SI B., LV J., WANG J. Evaluation of 14 frozen soil thermal conductivity models with observations and SHAW model simulations. Geoderma. **403**, 115207, **2021**.
80. KOJIMA Y., HEITMAN J.L., FLERCHINGER G.N., HORTON R. Numerical Evaluation of a Sensible Heat Balance Method to Determine Rates of Soil Freezing and Thawing. Vadose Zone Journal. **12** (1), 1, **2013**.
81. YANG Y., CHEN R., YE B., SONG Y., LIU J., HAN C., LIU Z. Heat and Water Transfer Processes on the Typical Underlying Surfaces of Frozen Soil in Cold Regions (II): Water and Heat Transfer. Journal of Glaciology and Geocryology. **35** (6), 1555, **2013** [In Chinese].
82. CHEN J., GAO X., ZHENG X., MIAO C., ZHANG Y., DU Q., XU Y. Simulation of Soil Freezing and Thawing for Different Groundwater Table Depths. Vadose Zone Journal. **18** (1), 1, **2019**.
83. P. E.J. CoupModel: Model Use, Calibration, and Validation. Transactions of the ASABE. **55** (4), 1337, **2012**.
84. HU G., ZHAO L., LI R., WU T., WU X., PANG Q., XIAO Y., QIAO Y., SHI J. Modeling hydrothermal transfer processes in permafrost regions of Qinghai-Tibet Plateau in China. Chinese Geographical Science. **25** (6), 713, **2015**.
85. WAN H., BIAN J., ZHANG H., LI Y. Assessment of future climate change impacts on water-heat-salt migration in unsaturated frozen soil using CoupModel.

Frontiers of Environmental Science & Engineering. **15** (1), 10, **2021**.
86. HU G., ZHAO L., WU X., LI R., WU T., XIE C., PANG Q., XIAO Y., LI W., QIAO Y., SHI J. Modeling permafrost properties in the Qinghai-Xizang (Tibet) Plateau. Science China-Earth Sciences. **58** (12), 2309, **2015**.
87. CONRAD Y., FOHRER N. A test of CoupModel for assessing the nitrogen leaching in grassland systems with two different fertilization levels. Journal of Plant Nutrition and Soil Science. **172** (6), 745, **2009**.
88. ZHAO Y., NISHIMURA T., HILL R., MIYAZAKI T. Determining Hydraulic Conductivity for Air-Filled Porosity in an Unsaturated Frozen Soil by the Multistep Outflow Method. Vadose Zone Journal. **12** (1), 1, **2013**.
89. FU C., XUE J., CHEN J., CUI L., WANG H. Evaluating spatial and temporal variations of soil water, heat, and salt under autumn irrigation in the Hetao Irrigation District based on distributed SHAW model. Agricultural Water Management. **293**, 108707, **2024**.
90. WANG L., ZHOU J., QI J., SUN L., YANG K., TIAN L., LIN Y., LIU W., SHRESTHA M., XUE Y., KOIKE T., MA Y., LI X., CHEN Y., CHEN D., PIAO S., LU H. Development of a land surface model with coupled snow and frozen soil physics. Water Resources Research. **53** (6), 5085, **2017**.
91. BAO H., KOIKE T., YANG K., WANG L., SHRESTHA M., LAWFORD P. Development of an enthalpy-based frozen soil model and its validation in a cold region in China. Journal of Geophysical Research-Atmospheres. **121** (10), 5259, **2016**.
92. ZHOU J., WEI C., LI D., WEI H. A moving-pump model for water migration in unsaturated freezing soil. Cold Regions Science and Technology. **104-105**, 14, **2014**.
93. GARAYSHIN V.V., NICOLSKY D.J., ROMANOVSKY V.E. Numerical modeling of two-dimensional temperature field dynamics across non-deforming ice-wedge polygons. Cold Regions Science and Technology. **161**, 115, **2019**.
94. PENG Z., TIAN F., WU J., HUANG J., HU H., DARNAULT C.J.G. A numerical model for water and heat transport in freezing soils with nonequilibrium ice-water interfaces. Water Resources Research. **52** (9), 7366, **2016**.
95. YU L., ZENG Y., WEN J., SU Z. Liquid-Vapor-Air Flow in the Frozen Soil. Journal of Geophysical Research-Atmospheres. **123** (14), 7393, **2018**.
96. WANG Z., PAN L., WANG L., WANG H. Urchin-like CdS microspheres self-assembled from CdS nanorods and their photocatalytic properties. Solid State Sciences. **13** (5), 970, **2011**.
97. WANG Y., ZHANG C., HU J., ZHANG P., ZHANG L., LAO L. Investigation on calendar experiment and failure mechanism of lithium-ion battery electrolyte leakage. Journal of Energy Storage. **54**, 105286, **2022**.
98. YOU C., FAN W., XIONG X., YANG H., FU L., WANG T., WANG F., ZHU Z., HE J., WU Y. Design Strategies for Anti-Freeze Electrolytes in Aqueous Energy Storage Devices at Low Temperatures. Advanced Functional Materials. **34** (40), 2403616, **2024**.